[CANCER RESEARCH 64, 5982–5987, September 1, 2004]

Inverse Correlation between Cyclin A1 Hypermethylation and p53 Mutation in Head and Neck Cancer Identified by Reversal of Epigenetic Silencing

Yutaka Tokumaru,[1] Keishi Yamashita,[1] Motonobu Osada,[1] Shuji Nomoto,[1] Dong-Il Sun,[3] Yan Xiao,[1] Mohammad Obaidul Hoque,[1] William H. Westra,[2] Joseph A. Califano,[1] and David Sidransky[1]

[1]Department of Otolaryngology–Head and Neck Surgery, Head and Neck Cancer Research Division and [2]Department of Pathology, Johns Hopkins University School of Medicine, Baltimore, Maryland; and [3]Department of Otolaryngology-Head and Neck Surgery, College of Medicine, The Catholic University of Korea, Seoul, Korea

ABSTRACT

Aberrant promoter hypermethylation of tumor suppressor genes is proposed to be a common feature of primary cancer cells. We recently developed a pharmacological unmasking microarray approach to screen unknown tumor suppressor gene candidates epigenetically silenced in human cancers. In this study, we applied this method to identify such genes in head and neck squamous cell carcinoma (HNSCC). We identified 12 novel methylated genes in HNSCC cell lines, including PGP9.5, cyclin A1, G0S2, bone-morphogenetic protein 2A, MT1G, and neuromedin U, which showed frequent promoter hypermethylation in primary HNSCC (60%, 45%, 35%, 25%, 25%, and 20%, respectively). Moreover, we discovered that cyclin A1 methylation was inversely related to p53 mutational status in primary tumors ($P = 0.015$), and forced expression of cyclin A1 resulted in robust induction of wild-type p53 in HNSCC cell lines. Pharmacological unmasking followed by microarray analysis is a powerful tool to identify key methylated tumor suppressor genes and relevant pathways.

INTRODUCTION

Head and neck cancer represents the sixth most frequent cancer in the world and at least 90% are squamous cell carcinomas (1). Head and neck cancer patients with early-stage are often asymptomatic, resulting in delayed diagnosis and advanced-stage, thus the overall survival rate is one of the lowest of the major cancers and has not improved significantly during the last decades.

Molecular approaches have elucidated the molecular genetic changes in head and neck squamous cell carcinoma (HNSCC) progression (2). Loss of chromosomal region 9p21 and inactivation of the p16 gene are the most common genetic changes and occur early in the progression of HNSCC (3). Approximately half of all head and neck cancers also contain a mutation of the p53 gene located at 17p13 (4). In addition, epigenetic pathways are presumed to play a significant role in silencing of tumor suppressor genes (TSGs) during human carcinogenesis. Epigenetic transcriptional silencing by promoter hypermethylation of TSGs is thought to be a common feature of human cancer (5, 6). Several critical TSGs epigenetically silenced in specific cancers have been reported, including RAS association domain family 1A gene in lung cancer (7), opioid binding protein/cell adhesion molecule like (OPCML) gene in ovarian cancer (8) and RUNX3 in gastric cancer (9). Although some methylated genes have been reported in HNSCC, including p16, O^6-methylguanine-DNA methyltransferase (4), death-associated protein kinase (10) and RAS association domain family 1A gene (11), they all occur in <33% of primary tumors. Therefore there is a need to characterize more methylated targets and identify more prevalent epigenetically silenced TSGs in HNSCC.

Oligonucleotide microarray-based analysis is an emerging technology for genome-wide detection that has opened up new possibilities in epigenetic research. We recently described a pharmacological unmasking microarray approach based on application of the demethylating agent, 5-aza-2′-deoxycytidine (5Aza-dC), and histone deacetylase inhibitor, trichostatin A (TSA) to cancer cell lines followed by hybridization of cRNA containing re-expressed genes to standard microarrays (12). In the present study, we applied this pharmacological unmasking microarray approach to HNSCC to comprehensively identify common epigenetically silenced genes. Through this high-throughput screening approach, we identified many novel methylated TSG candidates, some of which showed frequent hypermethylation specific to primary tumors. Moreover, we discovered a unique inverse relationship between cyclin A1-promoter hypermethylation and p53 mutation in these tumors.

MATERIALS AND METHODS

Cell Lines and Tissue Samples. HNSCC cell lines, 011, 012, 013, 019, 022, and 028 were established in Johns Hopkins University, Department of Otolaryngology-Head and Neck Surgery (Baltimore, MD) and FADU was obtained from the American Type Culture Collection (Manassas, VA). 011, 012, 013, 019, 022, and 028 cells were grown in RPMI 1640 (Invitrogen, Carlsbad, CA) supplemented with 10% fetal bovine serum (Hyclone, Logan, UT) and FADU cells in MEM (Invitrogen) with 10% fetal bovine serum. In all, 39 primary HNSCC tissues were obtained from surgical specimens resected at the Johns Hopkins University Hospital. We used 11 oral epithelium tissue samples from healthy non-smoking individuals as normal controls. Tumor DNA was prepared as described previously (13). P53 mutational status of these tumor samples was analyzed as described previously (14).

5Aza-dC and TSA Treatment of Cells. We treated HNSCC cell lines with 5Aza-dC and/or TSA as described previously (12). Briefly cells were split to low density (1×10^6 cells/T-75 flask) 24 hours before treatment. Stock solutions of 5Aza-dC (Sigma, St. Louis, MO) and TSA (Sigma) were dissolved in DMSO (Sigma) and 100% ethanol, respectively. Cells were treated with 0.2 or 2 mmol/L 5Aza-dC for 5 days and/or 300 nmol/L TSA for last 24 hours. We also mock-treated cells with the same volume of DMSO or ethanol.

Oligonucleotide Microarray Analysis and RT-PCR Analysis. Total cellular RNA was isolated using the RNeasy kit (Qiagen, Valencia, CA) according to the manufacturer's instruction. We carried out oligonucleotide microarray analysis using the GeneChip Human Genome U95Av2 Array (Affymetrix, Santa Clara, CA) as described previously (12). Signal intensity for each transcript was analyzed using the Microarray Suite Softwear 5.0 (Affymetrix). We used a 3-fold increase cutoff value after 5Aza-dC and/or TSA treatment to identify candidate genes.

Total RNA was measured and adjusted to the same amount for each cell line, and then cDNA synthesis was performed using random hexamers with the SuperScript First-Strand Synthesis kit (Invitrogen). The final cDNA products

Received 3/23/04; revised 5/28/04; accepted 6/20/04.

Grant Support: National Institutes of Health Grants UO1 CA 98-028, RO1 DE13561-01, and P50-CA96784 and Oncomethylome Sciences, SA.

The costs of publication of this article were defrayed in part by the payment of page charges. This article must therefore be hereby marked *advertisement* in accordance with 18 U.S.C. Section 1734 solely to indicate this fact.

Note: Under a licensing agreement between Oncomethylome Sciences, SA and the Johns Hopkins University, Dr. Sidransky is entitled to a share of royalty received by the University on sales of products described in this article. Dr. Sidransky owns Oncomethylome Sciences, SA stock, which is subject to certain restrictions under University policy. Dr. Sidransky is a paid consultant to Oncomethylome Sciences, SA and is a paid member of the company's Scientific Advisory Board. The terms of this arrangement are being managed by the Johns Hopkins University in accordance with its conflict of interest policies.

Requests for reprints: David Sidransky, Head and Neck Cancer Research Division, The Johns Hopkins University School of Medicine, 818 Ross Research Building, 720 Rutland Avenue, Baltimore, MD 21205-2196. Phone: 410-502-5153; Fax: 410-614-1411, E-mail: dsidrans@jhmi.edu.

were used as the templates for subsequent PCR with primers designed specifically for each candidate gene. Glyceraldehyde-3-phosphate dehydrogenase was examined to ensure accurate relative quantitation in PCR. The PCR products were resolved by agarose gel and visualized with ethidium bromide staining. Detailed PCR conditions and primer sequences are available upon request.

Any gene determined to be up-regulated after 5Aza-dC treatment was notated. We then selected commonly up-regulated genes that occurred in two or more cell lines. Reverse-transcription (RT)-PCR did not always confirm up-regulation, because of hybridization errors in the microarray analysis.

Bisulfite Genomic Sequence Analysis. Bisulfite sequence analysis was performed to check the methylation status in cell lines and clinical samples. We extracted genomic DNA and carried out bisulfite modification of genomic DNA as described previously (15).

Bisulfite-treated DNA was amplified for the 5′ region that included the proposed transcriptional start site using primer sets. The primers were designed from regions in which there are no CpG dinucleotides. Detailed primer sequences and PCR conditions are available upon request. The PCR products were gel-purified using the QIAquick Gel Extraction Kit (Qiagen) according to the manufacturer's instructions. Each amplified DNA sample was applied with nested primers to the Applied Biosystems 3700 DNA analyzer using BD terminator dye (Applied Biosystems, Foster City, CA).

Immunohistochemical Analysis of Cyclin A1 and p53. Four micrometer-thick sections sliced from paraffin-embedded HNSCC specimens were deparaffinized by xylene and subjected to antigen retrieval by microwaving in 10 mmol/L of sodium citrate for 30 minutes. The sections were incubated with a mouse monoclonal antihuman cyclin A antibody (6E6, Novocastra Laboratory, Newcastle United Kingdom) and with a mouse monoclonal anti-p53 antibody (Ab-8, Neomarker, Fremont, CA) for 12 to 16 hours at 4°C and stained by EnVision+System (DAKO, Carpinteria, CA).

Transfection of Human Expression Vectors and Western Blotting. A full-length cDNA of cyclin A1 was isolated from HNSCC cell line 012 using PCR with the primer sets 5′-AAAAAGCTTCCACCATGGAGACCGGCTTTCCCGCAATC-3′ and 5′-TTTTCTAGATTGTAGAAGAAGAACTGCAGGTGGC-3′. The PCR products were cut with *Hind*III and *Xba*I and ligated to *Hind*III-*Xba*I digested p3xFLAG-CMV (Sigma). HNSCC cell lines (019, 022, 028, and Fadu) were plated at 2×10^5/well using 6-well plates and transfected with either p3xFLAG-CMV-cyclin A1 or no insert of p3xFLAG-CMV-mock using the FuGene 6 Transfection Reagent (Roche, Basel, Switzerland) according to the manufacturer's protocol. After 2 days of transfection, cells were washed with PBS and suspended in 200 μl of RIPA buffer (50 mmol/L Tris-HCl (pH 7.5), 150 mmol/L NaCl/1% NP40/0.5% sodium deoxycholate/0.1% SDS) containing 1 mmol/L phenylmethylsulfonyl fluoride. The cells were incubated on ice for 20 minutes and then scraped. The lysate was then centrifuged at 10,000 rpm for 10 minutes, and supernatant was stored at −80°C. Western blotting was performed as described previously (16). The blot was incubated with anti-p53 antibody (Neomarker), anti-FLAG M2 antibody (Sigma), and anti-β-actin (Sigma) for 1 hour at room temperature and then incubated with peroxidase-conjugated sheep antimouse antibody (Amersham Biosciencies, Piscataway, NJ) for 1.5 hours. After washing, an ECL kit (Amersham Biosciencies) was used to visualize the antibody binding to each protein.

Statistical Analysis. Statistical significance of the prevalence of cyclin A1 methylation and p53 mutation was assessed by Fisher's exact test.

RESULTS

Pharmacological Unmasking Followed by cRNA Microarray. We treated HNSCC cell lines, 011 and 013, with 2 μmol/L 5Aza-dC for 5 days or 0.2 μmol/L 5Aza-dC for 5 days plus 300 nmol/L TSA for the last 24 hours to reactivate epigenetically silenced genes. Then we extracted total RNA from these cell lines and compared gene expressions profiles between mock and 5Aza-dC and/or TSA-treated cells by microarray chips. We first selected 278 commonly up-regulated genes in both 011 and 013 after treatment (up-regulation was defined as a 3-fold increase compared with mock; Fig. 1). We reduced the number of the candidate genes to 140 genes by expression profile analysis. This analysis was based on comparison of expression patterns[4] in HNSCC and normal tissue followed by elimination of genes not expressed in normal tissue and unknown genes. We then selected 53 genes with dense CpG sites (CpG > 15% or GC-rich > 60% over 50 bp) in the promoter region to focus on those most likely to be inactivated by promoter hypermethylation (Fig. 1).

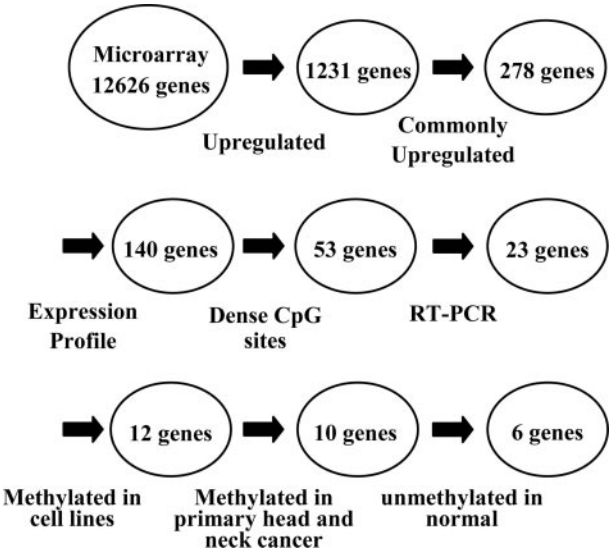

Fig. 1. Flowchart for selection of epigenetically silenced candidate TSGs in HNSCC. We treated HNSCC cell lines, 011 and 013, with 0.2 or 2 μmol/L 5Aza-dC and/or 300 nmol/L TSA to reactivate epigenetically silenced genes. We first selected 278 genes commonly up-regulated (>3.0-fold increase) after pharmacological unmasking. We reduced the number of the candidate genes to 140 by expression profile, based on database analysis of expression patterns in normal and tumor tissues. We finally selected 53 genes with dense CpG sites and investigated the expression of all of these genes by RT-PCR in seven HNSCC cell lines. We found that 23 of those 53 genes were completely silenced in at least one of the cell lines. Next we examined methylation status in the promoter region of these 23 genes by bisulfite sequencing. Among these 23 genes, 12 were methylated in at least one of the HNSCC cell lines. We then investigated methylation of these 12 genes in primary HNSCC tissues and normal samples by bisulfite sequence analysis. Ten genes were methylated in primary HNSCC and only six were specifically methylated in tumor and yet remained unmethylated in normal samples.

Gene Reactivation and Promoter Hypermethylation in HNSCC Cell Lines. We investigated expression of the 53 genes described above by RT-PCR using seven HNSCC cell lines before and after pharmacological unmasking (Table 1; representative results are shown in Fig. 2*A*). Among these 53 genes, 23 were completely silenced in at least one of the seven HNSCC cell lines. The remaining 30 genes showed baseline expression and increased expression after treatment. We previously reported that most of the latter genes with baseline expression are eventually found to lack promoter methylation (12). We thus examined the methylation status in the promoter region of the 23 genes with no baseline expression using bisulfite sequencing (Table 1). Among these 23 genes, 12 were methylated in at least one of the seven HNSCC cell lines (Fig. 2*B* and representative results were shown in Fig. 2*C*), and this methylation status was completely consistent with gene expression by RT-PCR.

Promoter Hypermethylation in Primary HNSCC Tumors. The methylation status of cancer cell lines does not always reflect the prevalence of methylation in primary tumors. We investigated the promoter methylation status of these 12 genes in 20 primary HNSCC tissues and 11 normal samples by bisulfite sequence analysis. Ten genes were methylated in primary HNSCC (Table 1); however, only six genes [protein gene product 9.5, PGP9.5; cyclin A1, G_0/G_1 switch gene 2, G0S2; metallothionein 1G, MT1G; bone-morphogenetic protein 2A, bone morphogenetic protein 2A (BMP2A); and neuromedin

[4] http://cgap.nci.nih.gov.

Table 1 *Candidate methylated genes in HNSCC*

Genebank accession no.	Gene name	Gene expression*		Methylation in cell lines‡	Methylation in tissue‡	
		Before treatment†	After treatment†		Primary ca§	Normal
AB023211	Arginine deiminase (PADI2)	(+)	(++)			
M69199	G0S2 protein	(−)	(+)	(+)	(+)	(−)
D13891	Inhibitor of DNA binding 2, ID-2	(−)	(−)	(−)		
M59287	CDC-like kinase 1, CLK1	(−)	(+)	(−)		
AI743134	Protease inhibitor 7, Nexin	(+)	(++)			
X02761	Fibronectin	(+)	(++)			
Z81326	Protease inhibitor 12	(+)	(++)			
X04741	PGP 9.5	(−)	(+)	(+)	(+)	(−)
X76029	Neuromedin U	(−)	(+)	(+)	(+)	(−)
J02966	Solute carrier family 25, Member 4	(+)	(++)			
U03106	p21	(+)	(++)			
AL022723	Major histocompatibility complex I	(−)	(+)	(+)	(+)	(+)
Y10032	Serine/threonine protein kinase	(+)	(++)			
M73780	Integrin β-8	(−)	(−)	(+)	(−)	
AB001325	Aquaporine 3	(-)	(+)	(+)	(−)	
AB001928	Cathepsin V	(−)	(+)	(−)		
X04412	Plasma gelsolin	(+)	(++)			
D87258	Serin protease with IGF-binding motif	(−)	(−)	(−)		
U15932	Dual-specificity phosphatase 5, DUSP5	(+)	(++)			
U53831	Interferon regulatory factor 7B	(−)	(+)	(−)		
M13755	Interferon-induced 15-kDa protein (IFI-15k)	(−)	(+)	(−)		
AA883502	Ubiquitin-conjugating enzyme (UBCH8)	(+)	(++)			
X15675	pTR7	(+)	(++)			
AF095448	Retinoic acid-inducible gene 1(RAIG1)	(+)	(++)			
M26326	Keratin 18	(+)	(++)			
U50529	BRCA2	(+)	(++)			
U66838	Cyclin A1	(−)	(+)	(+)	(+)	(−)
M97935	Interferon-stimulated gene factor 3 (ISGF-3)	(+)	(++)			
AI670788	Modulator of apoptosis 1	(+)	(++)			
Y09568	Synaptosomal-associated Protein 23-kDa	(−)	(−)	(−)		
D28364	Annexin II	(+)	(++)			
AB002305	Aryl hydrocarbon receptor translocator 2	(+)	(++)			
X04434	Insulin-like growth factor I receptor	(+)	(++)			
X69433	Isocitrate dehydrogenase 2 (IDH2)	(−)	(+)	(−)		
J03910	Metallothionein-IG (MT1G)	(−)	(+)	(+)	(+)	(−)
AB014515	Nedd 4 binding protein	(+)	(++)			
AA224832	Metallothionein 1L, MT1L	(+)	(++)			
W26496	SOCS box containing WD-protein	(+)	(++)			
M62403	Insulin-like growth factor binding protein 4	(+)	(++)			
S69189	Peroxisomal acyl-coenzyme A oxidase	(+)	(++)			
U03398	Tumor necrosis factor ligand 9	(+)	(++)			
J03909	γ-interferon-inducible protein (IP-30)	(+)	(++)			
M92843	Zing finger protein 36	(+)	(++)			
U87947	Epithelial membrane protein 3 (EMP3)	(−)	(+)	(+)	(+)	(+)
AA152406	Cytochrome *c* oxidase polypeptide VIIA-heart	(−)	(−)	(+)	(+)	(+)
M22489	Bone morphogenetic protein 2A (BMP2A)	(−)	(+)	(+)	(+)	(−)
M55153	Transglutaminase (TGase) 2	(+)	(++)			
X63187	HE4 (WAP four-disulfide core domain2)	(−)	(+)	(+)	(+)	(+)
D79206	Ryudocan, Syndecan 4	(−)	(+)	(−)		
L13286	Cytochrome P450 superfamily XXIV	(+)	(++)			
Y07593	Coxsackievirus and adenovirus receptor	(−)	(−)	(−)		
AF049891	Tyrosylprotein sulfotransferase-2	(−)	(+)	(−)		
AF063002	LIM protein SLIMMER	(+)	(++)			

* Gene expression in HNSCC cell lines by RT-PCR, if at least one of the cell lines showed little or no expression before 5Aza-dC treatment and reactivation after treatment, the expression pattern for the gene of interest was included.

† Before and after 5Aza-dC treatment.

‡ Methylation analysis by bisulfite sequencing.

§ Primary HNSCC tissue.

U] were methylated in a tumor-specific manner (Fig. 3*A*; representative results are shown in Fig. 3*B*). The frequency of methylation in primary tumors was 60% for PGP9.5, 45% for cyclin A1, 35% for G0S2, 25% for BMP2A, 25% for MT1G, and 20% for neuromedin U. MHC class I, EMP-3, Cox7A1, and HE-4 were methylated in both normal tissues and primary tumors.

Hypermethylation of Cyclin A1 and p53 Mutation. We were intrigued to discover tumor-specific methylation of cyclin A1 in 45% of primary HNSCCs. Cyclin A1 is known to be downstream of p53 (17), a known component of growth arrest and apoptosis in certain circumstances (18–20). We thus decided to investigate the relationship between cyclin A1 methylation status and p53 mutational status in 39 primary HNSCC tissues. Surprisingly, cyclin A1 methylation status showed a marked inverse correlation with p53 mutational status (Table 2). Cyclin A1 was clearly more frequently hypermethylated in primary tumor tissues with wild-type p53 status (11 of 19, 58%) as compared with methylation in those with mutant status (4 of 20, 20%; $P = 0.015$). Furthermore, quantitative analysis of cyclin A1 in these latter four samples showed only minimal methylation by real-time methylation-specific PCR (ref. 21; data not shown). This finding confirmed selective pressure against cyclin A1 expression in p53 wild-type but not p53 mutant cells.

Expression of Cyclin A1 and p53 in Primary HNSCC Tissue. Representative results of immunohistochemistry of cyclin A1 and p53 in primary HNSCC tissues are shown in Fig. 4. Staining for both gene products was localized to the nucleus of tumor cells. Overexpression of p53 protein was found in primary HNSCC with mutant p53 status as expected (Fig. 4*B*). Bisulfite sequence analysis revealed absence of cyclin A1 methylation in this tumor, and cyclin A1 protein was expressed robustly (Fig. 4*C*). On the other hand, p53 protein was not

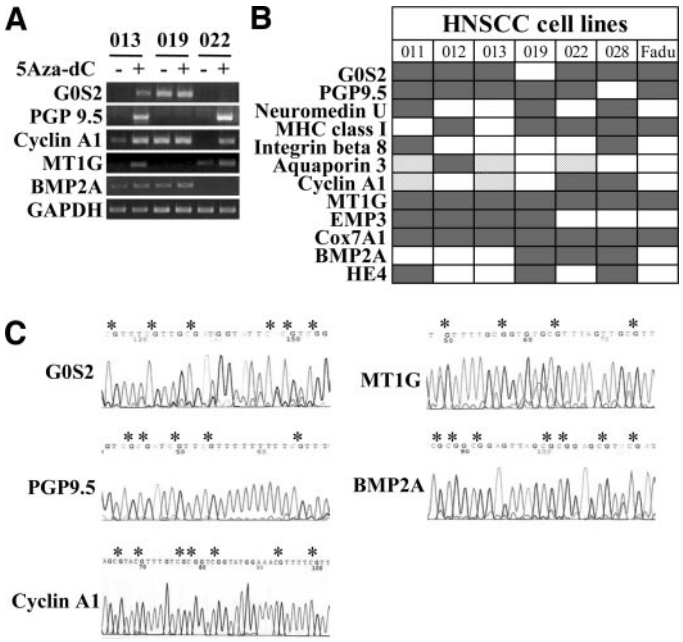

Fig. 2. Methylation and gene expression in HNSCC cell lines. *A*, RT-PCR analysis of five genes in representative three HNSCC cell lines. All cell lines were treated with (+) or without (−) 5Aza-dC. *B*, summary of methylation profiles of 12 methylated genes in seven HNSCC cell lines. *Filled boxes* indicate methylation and *light speckled boxes* indicate partial methylation by bisulfite sequence analysis. *C*, bisulfite sequence analysis of the five representative genes methylated in HNSCC cell lines. G0S2 (013), PGP9.5 (022), cyclin A1 (028), MT1G (013), and BMP2A (022). Asterisks (*) indicate methylated CpG sites in each gene sequence.

detected in a p53 wild-type tumor (Fig. 4*E*), and cyclin A1 expression was nearly absent in this sample because of hypermethylation of cyclin A1 (Fig. 4*F*). These results further support the inverse correlation between cyclin A1 and p53 shown in Table 2.

Cyclin A1 Induced p53 in HNSCC Cell Lines with Wild-Type p53. We then made a cyclin A1 cDNA construct with a cytomegalovirus (CMV) promoter and transfected the plasmid into four HNSCC cell lines to examine the effect of forced cyclin A1 expression on the p53 pathway. Transient expression of cyclin A1 clearly induced p53 protein in p53 wild-type HNSCC cells (022 and 028; Fig. 5*A*) but not in cells with mutant p53 (019 and Fadu). These results suggest that cyclin A1 is involved in p53 induction and thus possesses a potential suppressive role in HNSCC carcinogenesis. Combined with previous data demonstrating induction of cyclin A1 by wild-type p53, we propose a positive feedback loop between cyclin A1 and p53 that is abrogated in HNSCC by p53 mutation or silencing of cyclin A1 expression through promoter hypermethylation (Fig. 5*B*).

DISCUSSION

Until recently, most methylated targets were identified by laborious testing using one gene at a time. Our pharmacological treatment and microarray approach allows rapid and comprehensive screening of multiple gene promoters in cancer cell lines. Using microarray data after treatment to assess reversal of epigenetic silencing and using direct sequencing to validate the presence of methylation, we identified six cancer-specific methylated genes in primary HNSCC samples. Each of these genes is now a molecular marker for diagnostic and therapeutic approaches in human cancers (22).

From our previous experiments (12), we noticed that the pharmacological unmasking up-regulated many genes without DNA hypermethylation, because these genes might be downstream of true epigenetically silenced genes in cancer cell lines. We found that complete silencing of expression before treatment is a useful landmark to identify genes with DNA hypermethylation. Fifteen of 32 completely silenced genes (55%) in our previous results in esophageal squamous cell carcinoma (12) and 12 of 23 (52%) in this study in HNSCC were found to be methylated. Thus, we believe RT-PCR is very effective for further screening in that it distinguishes complete silencing of gene expression from very low expression levels. Indeed, we ruled out 30 genes among 53 candidates by initial RT-PCR. The pharmacological unmasking approach still has some weak points. For example, we did not observe up-regulation of some genes previously reported as meth-

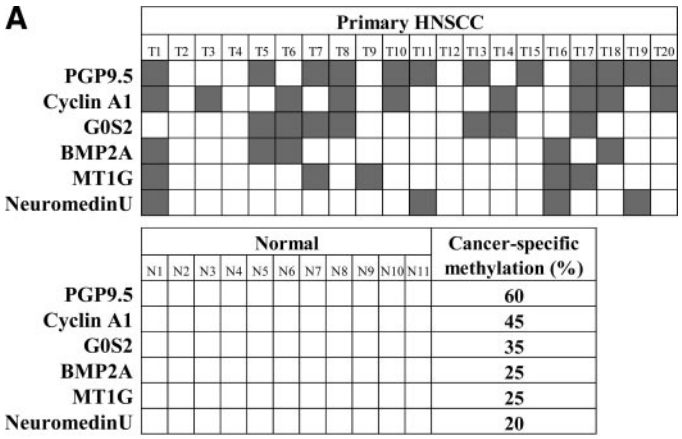

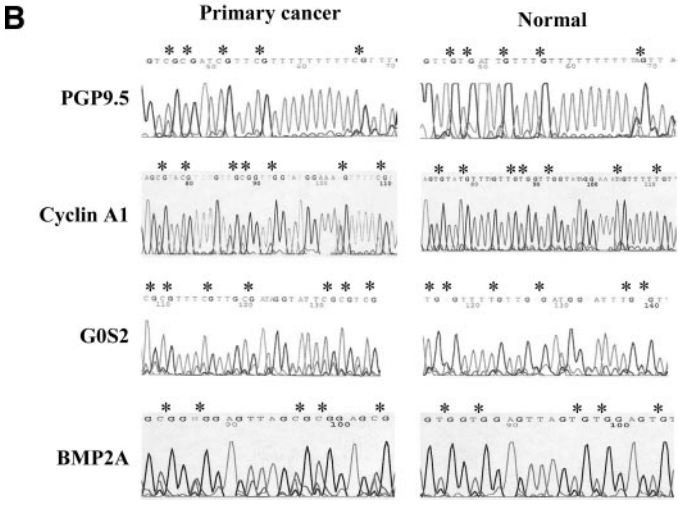

Fig. 3. Cancer-specific hypermethylation in primary HNSCC tissue. *A*, summary of methylation profiles of six cancer-specific methylated genes in primary HNSCC tissues. These six genes were methylated in primary tumor but not methylated in normal samples, suggesting cancer specific hypermethylation. *Filled boxes* indicate methylation; *open boxes* indicate absence of methylation by bisulfite sequence analysis. *B*, bisulfite sequence analysis of the four representative genes methylated in primary HNSCC tissue. Asterisks (*) indicate CpG islands in each gene. After bisulfite treatment, methylated CpGs are protected, whereas unmethylated CpGs are converted to TGs. These six genes showed cancer-specific hypermethylation in primary HNSCC tissues.

Table 2 *Cyclin A1 promoter hypermethylation and p53 mutational status in HNSCC*

		p53 mutational status	
		Wild-type	Mutant type
Cyclin A1 methylation status	Methylated	11*	4†
	Unmethylated	8	16‡

* Immunohistochemistry (IHC) was done in six cases and four of these cases showed little or no expression of cyclin A1. The remaining two cases showed weak staining in <30% of cells.

† Methylation present in <10% alleles.

‡ IHC was done in five cases and all cases showed robust expression of cyclin A1.

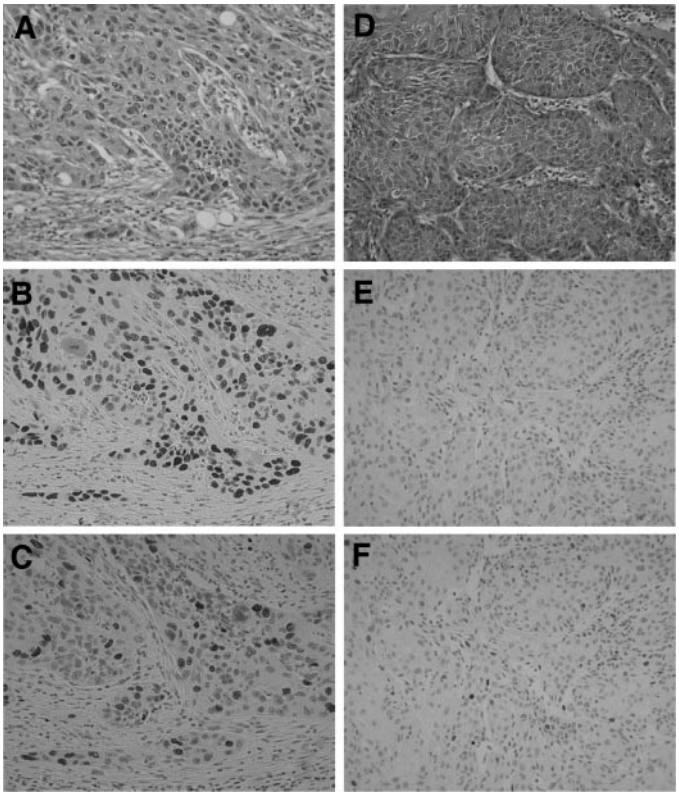

Fig. 4. Representative results of immunohistochemistry of cyclin A1 and p53 in HNSCC primary cancer with mutant type p53 (*A*, *B*, *C*) and with wild type p53 (*D*, *E*, *F*). Dense p53 staining was detected in mutant-type p53 cancer tissue (*B*) but not in wild-type tissue (*E*). Cyclin A1 protein was detected robustly in mutant-type p53 cancer tissue (C) in the absence of cyclin A1 methylation in this sample. Cyclin A1 expression was markedly weak in mutant-type p53 cancer tissue (*F*) associated with hypermethylation of cyclin A1. H&E staining was performed for reference (*A*, *D*).

ylated such as p16. This might be the limitation of microarray detection for genes with very low level expression and the use of only 2 cell lines. More robust demethylation could also be achieved by further combination of demethylating agents and HDAC inhibitors or by a more sensitive approach such as differential cloning (23). Moreover, additional microarray algorithms are needed to more quickly focus screening efforts on the best candidate genes.

Among the new methylated genes in HNSCC, we previously identified methylation of MT1G and neuromedin U in esophageal squamous cell carcinoma (12). PGP9.5 showed the highest frequency of cancer-specific methylation in this study of head and neck cancer. PGP9.5 is a neuro-specific peptide that functions to remove ubiquitin from ubiquitinated proteins and prevents them from targeted degradation by proteasomes (24). Serial analysis of gene expression analysis identified PGP9.5 overexpression in lung carcinoma; however, half of the primary tumors displayed absent expression (25). One recent study revealed a high prevalence of PGP9.5 methylation in pancreatic cancer (26). Taken together, we propose that PGP9.5 is silenced by hypermethylation in many cancers and might function as a tumor suppressor gene in these tumors.

Other identified methylated genes such as G0S2 and BMP2A provide intriguing insight into tumor suppression. Early mRNA expression of G0S2 is inhibited by cyclosporin A, which also inhibits Ca2+-mediated up-regulation of the DNA repair enzyme DNA polymerase β in human peripheral blood mononuclear cells (27). G0S2 may thus directly augment the DNA repair system in human cells. BMP2A is part of the BMP family, which belongs to the transforming growth factor-β superfamily. Recently, BMP1 mutations were found in patients with juvenile polyposis, suggesting that BMP family members function as tumor suppressors (28). Furthermore, recent observations suggest that BMP2 mediates retinoid-induced apoptosis in medulloblastoma cells (29) and may be necessary and sufficient for apoptosis in retinoid-responsive cells.

The most interesting finding was the high frequency of cyclin A1 methylation in HNSCC. Cyclin A1 is a known down stream target of p53 (17). We investigated the relationship between cyclin A1 methylation and p53 mutational status in primary HNSCC and found an intriguing reciprocal correlation, suggesting that cyclin A1 expression is not tolerated in tumors when p53 is in a wild-type state. Furthermore, we demonstrated that cyclin A1 induced p53 in HNSCC cell lines with wild-type p53 but not in cells with mutant p53. This induction of p53 could be caused by a variety of mechanisms, directly or indirectly, which need to be explored in much greater detail. However these results are supported by a recent report (30), suggesting that cyclin A1 is involved in repression of DNA rereplication by p21 induction through p53.

Cyclin family members are well-known molecules that play a relevant role in cell cycle progression and are often overexpressed in a subset of cancer tissues (31). On the other hand, there have been several reports describing the involvement of cyclin A1 in growth arrest and apoptosis. Meikrantz *et al.* showed that cyclin A1 induced apoptosis in HeLa cells after exposure to chemical agents and that the induction of apoptosis was accompanied by cyclin A-dependent protein kinases. They suggested that cyclin A targets activated cell division cycle 2 and cyclin-dependent kinase 2 to substrates necessary

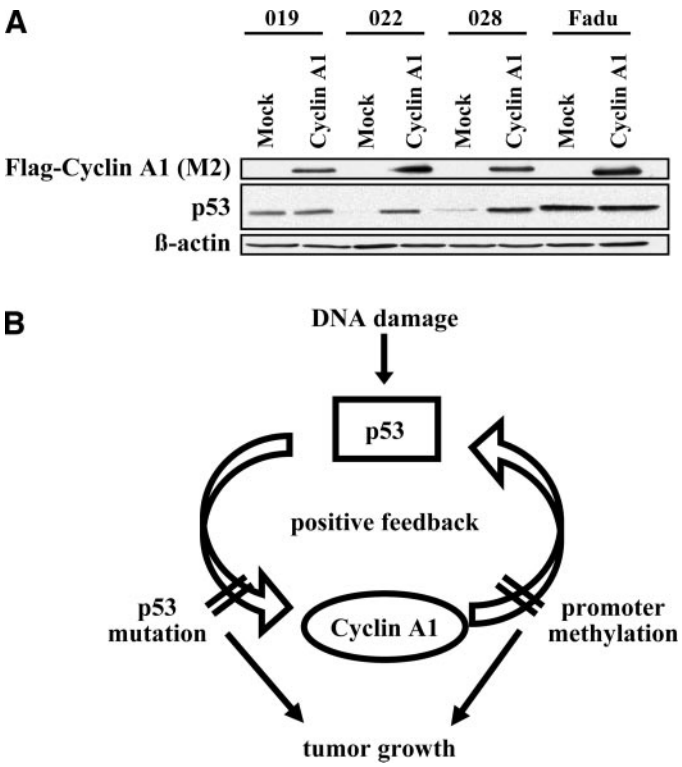

Fig. 5. Cyclin A1 induced p53 in HNSCC cell lines with p53 wild-type. *A*, p53 induction after cyclin A1 transient transfection in HNSCC cell lines with wild-type p53. A full-length cyclin A1 cDNA was cloned into p3xFLAG-CMV, and HNSCC cell lines (019, 022, 028, and Fadu) were transfected with either p3xFLAG-CMV-cyclin A1 or no insert p3xFLAG-CMV-mock. Western blotting was performed with anti-p53 antibody, anti-FLAG M2 antibody and anti-β-actin. Cyclin A1 induced p53 protein robustly in HNSCC cells with p53 wild-type (022 and 028) but not in cells with mutant p53 (019 and Fadu). B, proposed positive feedback model between p53 and cyclin A1. This pathway is abrogated in primary tumors through p53 mutation or methylation of the cyclin A1 promoter.

for chromatin condensation and other morphological changes during apoptosis (18). They also showed that cyclin A expression markedly elevated the level of apoptosis in BCL-2^+ cells (19). Others observed that cyclin A mRNA levels were elevated in cells undergoing apoptosis (20). In addition, they demonstrated that Zn^{2+}-inducible cyclin A expression was sufficient to cause apoptosis and apoptosis induced by c-Myc accompanied by elevated cyclin A mRNA levels. These results suggest that cyclin A1 possesses a growth-suppressive function in specific cellular contexts. The reciprocal relationship between cyclin A promoter methylation and p53 mutation suggests that these genes are in the same pathway. This relationship is reminiscent of independent antigen-presenting cells inactivation and β-catenin-activating mutations in colorectal carcinoma (32) or the inverse relationship between Ras and Raf mutations in primary colorectal carcinoma and lung cancer (33). Our results support the critical nature of the p53 pathway in HNSCC (2) and suggest that cyclin A1 may be an important amplification signal for p53 activity in HNSCC. Continued unmasking of genetically silenced genes is likely to identify new diagnostic and therapeutic targets in human cancers.

ACKNOWLEDGMENTS

We thank Yuichi Nagakawa for technical assistance.

REFERENCES

1. Jemal A, Thomas A, Murray T, Thun M. Cancer statistics, 2002. CA Cancer J Clin 2002;52:23–47.
2. Califano J, van der Riet P, Westra W, et al. Genetic progression model for head and neck cancer: implications for field cancerization. Cancer Res 1996;56:2488–92.
3. van der Riet P, Nawroz H, Hruban RH, et al. Frequent loss of chromosome 9p21–22 early in head and neck cancer progression. Cancer Res 1994;54:1156–8.
4. Somers KD, Merrick MA, Lopez ME, Incognito LS, Schechter GL, Casey G. Frequent p53 mutations in head and neck cancer. Cancer Res 1992;52:5997–6000.
5. Jones PA, Laird PW. Cancer epigenetics comes of age. Nat Genet 1999;21:163–7.
6. Baylin SB, Herman JG. DNA hypermethylation in tumorigenesis: epigenetics joins genetics. Trends Genet 2000;16:168–74.
7. Dammann R, Li C, Yoon JH, Chin PL, Bates S, Pfeifer GP. Epigenetic inactivation of a RAS association domain family protein from the lung tumour suppressor locus 3p21.3. Nat Genet 2000;25:315–9.
8. Sellar GC, Watt KP, Rabiasz GJ, et al. OPCML at 11q25 is epigenetically inactivated and has tumor-suppressor function in epithelial ovarian cancer. Nat Genet 2003;34:337–43.
9. Li QL, Ito K, Sakakura C, et al. Causal relationship between the loss of RUNX3 expression and gastric cancer. Cell 2002;109:113–24.
10. Sanchez-Cespedes M, Esteller M, Wu L, et al. Gene promoter hypermethylation in tumors and serum of head and neck cancer patients. Cancer Res 2000;60:892–5.
11. Hasegawa M, Nelson HH, Peters E, Ringstrom E, Posner M, Kelsey KT. Patterns of gene promoter methylation in squamous cell cancer of the head and neck. Oncogene 2002;21:4231–6.
12. Yamashita K, Upadhyay S, Osada M, et al. Pharmacologic unmasking of epigenetically silenced tumor suppressor genes in esophageal squamous cell carcinoma. Cancer Cell 2002;2:485–95.
13. Nawroz H, Koch W, Anker P, Stroun M, Sidransky D. Microsatellite alterations in serum DNA of head and neck cancer patients. Nat Med 1996;2:1035–7.
14. Koch WM, Brennan JA, Zahurak M, et al. p53 mutation and locoregional treatment failure in head and neck squamous cell carcinoma. J Natl Cancer Inst (Bethesda) 1996;88:1580–6.
15. Merlo A, Herman JG, Mao L, et al. 5′ CpG island methylation is associated with transcriptional silencing of the tumour suppressor p16/CDKN2/MTS1 in human cancers. Nat Med 1995;1:686–92.
16. Hibi K, Trink B, Patturajan M, et al. AIS is an oncogene amplified in squamous cell carcinoma. Proc Natl Acad Sci USA 2000;97:5462–7.
17. Maxwell SA, Davis GE. Differential gene expression in p53-mediated apoptosis-resistant vs. apoptosis-sensitive tumor cell lines. Proc Natl Acad Sci USA 2000;97:13009–14.
18. Meikrantz W, Gisselbrecht S, Tam SW, Schlegel R. Activation of cyclin A-dependent protein kinases during apoptosis. Proc Natl Acad Sci USA 1994;91:3754–8.
19. Meikrantz W, Schlegel R. Suppression of apoptosis by dominant negative mutants of cyclin-dependent protein kinases. J Biol Chem 1996;271:10205–9.
20. Hoang AT, Cohen KJ, Barrett JF, Bergstrom DA, Dang CV. Participation of cyclin A in Myc-induced apoptosis. Proc Natl Acad Sci USA 1994;91:6875–9.
21. Usadel H, Brabender J, Danenberg KD, et al. Quantitative adenomatous polyposis coli promoter methylation analysis in tumor tissue, serum, and plasma DNA of patients with lung cancer. Cancer Res 2002;62:371–5.
22. Sidransky D. Emerging molecular markers of cancer. Nat Rev Cancer 2002;2:210–9.
23. Suzuki H, Gabrielson E, Chen W, et al. A genomic screen for genes upregulated by demethylation and histone deacetylase inhibition in human colorectal cancer. Nat Genet 2002;31:141–9.
24. Wilkinson KD, Lee KM, Deshpande S, Duerksen-Hughes P, Boss JM, Pohl J. The neuron-specific protein PGP 9.5 is a ubiquitin carboxyl-terminal hydrolase. Science (Wash D C) 1989;246:670–3.
25. Hibi K, Westra WH, Borges M, Goodman S, Sidransky D, Jen J. PGP9.5 as a candidate tumor marker for non-small-cell lung cancer. Am J Pathol 1999;155:711–5.
26. Sato N, Fukushima N, Maitra A, et al. Discovery of novel targets for aberrant methylation in pancreatic carcinoma using high-throughput microarrays. Cancer Res 2003;63:3735–42.
27. Cristillo AD, Heximer SP, Russell L, Forsdyke DR. Cyclosporin A inhibits early mRNA expression of G0/G1 switch gene 2 (G0S2) in cultured human blood mononuclear cells. DNA Cell Biol 1997;16:1449–58.
28. Howe JR, Bair JL, Sayed MG, et al. Germline mutations of the gene encoding bone morphogenetic protein receptor 1A in juvenile polyposis. Nat Genet 2001;28:184–7.
29. Hallahan AR, Pritchard JI, Chandraratna RA, et al. BMP-2 mediates retinoid-induced apoptosis in medulloblastoma cells through a paracrine effect. Nat Med 2003;9:1033–8.
30. Vaziri C, Saxena S, Jeon Y, et al. A p53-dependent checkpoint pathway prevents rereplication. Mol Cell 2003;11:997–1008.
31. Weinberg RA. The retinoblastoma protein and cell cycle control. Cell 1995;81:323–30.
32. Sparks AB, Morin PJ, Vogelstein B, Kinzler KW. Mutational analysis of the APC/beta-catenin/Tcf pathway in colorectal cancer. Cancer Res 1998;58:1130–4.
33. Rajagopalan H, Bardelli A, Lengauer C, Kinzler KW, Vogelstein B, Velculescu VE. Tumorigenesis: RAF/RAS oncogenes and mismatch-repair status. Nature (Lond) 2002;418:934.